Electronic Supplementary Material (ESI) for RSC Advances.

Supporting Information

Qualitative and quantitative adsorption mechanisms of zinc ions from aqueous solutions onto dead carp derived biochar

Hong-tao Qiao[a], Yong-sheng Qiao[a], Xiao-hang Luo[a], Bao-wei Zhao[b *], Qiu-ying Cai[a]

[a]*Institute of Applied Chemistry & Department of Chemistry, Xinzhou Teachers University, Xinzhou 034000, China*

[b]*School of Environmental and Municipal Engineering, Lanzhou Jiaotong University, Lanzhou 730070, China*

First author: 469494248@qq.com

**Corresponding author.*

E-mail address: zhbw2001@sina.com (Baowei Zhao).

Biochar preparation and characteristics

In order to obtain the demineralized biochars, the original biochars was washed three times with 0.1 M HCl (the ratio of 1:50 *w*/*v*) in constant temperature oscillator (150 rpm, 25) for 1 h, and then the treated biochars was washed with distilled water in the sand core funnel with 0.45 um filter membrane until the pH value of the leaching solution remained constant. Subsequently, the demineralized biochars was dried at 75 ℃ for 12 h, crushed and passed through a 0.17 mm sieve (80 mesh), and labeled DCMB450, DCMB550, and DCMB650, respectively.

The yield of original biochars and demineralized biochars were calculated by the mass ratio before and after preparation. The Zeta potential of biochars was measured by a potential analyzer at 25 ^{o}C using distilled water as dispersant (Otsuka, hobriba SZ-100, Japan). The pH values of all biochars were measured by adding biochar to deionized water at the ratio of 1:20 *w*/*v* after shaken for 1 h at 150 rpm [1]. The pore volume, BET surface area and pore size of biochars were obtained by using a surface area and porosimetry analyzer (micromeritics, ASAP2020C, USA) via N_2 adsorption isotherm at 77 K with the Brunauer-Emmett-Teller equation. Total C, H, N, and O of biochars were analyzed in duplicate by an elemental analyzer (MicroCube, Elementar, Germany). Thermal analysis of biochars were obtained by using a thermogravimetric analyzer (STA449F5, Netzsch, Germany) with the temperature risen from 30 ^{o}C to 900 ^{o}C by a heating rate of 10 ^{o}C min^{-1} under an atmosphere of N_2. The surface structure and elemental composition of biochars were visualized by using a JSM-7800F SEM with EDS (Japan). The surface chemical composition was determined by X-ray diffraction (Haoyuan, DX2700B, China) and X-ray photoelectron spectroscopy (Thermo Scientific, ESCALAB 250Xi, USA). The surface functional groups of biochars were identified by Fourier transform infrared spectroscopy (FTIR) (Bruker, TENSOR 27, Germany) between wave numbers 4000 to 400 cm^{-1}.

Data analysis method for adsorption experiments

The adsorption amount (Q_t) of Zn^{2+} on biochars was calculated according to Eq. (1) [2]:

$$Q_t = \frac{(C_0 - C_t)V}{m} \tag{1}$$

where Q_t (mg g^{-1}) was the amount of Zn^{2+} adsorbed by biochars at time t; C_0 (mg L^{-1}) and C_t (mg L^{-1}) were the initial Zn^{2+} concentration and the Zn^{2+} concentration when the adsorption time was t, respectively; V (L) was the volume of Zn^{2+} solution; m (g) was the mass of biochars.

The pseudo first order equation (Eq. 2), the pseudo second order equation (Eq. 3), the Elovich equation (Eq. 4) and the intra-particle diffusion equation (Eq. 5) were used to fit the adsorption kinetics process of Zn^{2+} on biochars, and the expressions of the equations were described as follows [3-5]:

$$\frac{dQ_t}{dt} = k_1(Q_e - Q_t) \tag{2}$$

$$\frac{dQ_t}{dt} = k_2(Q_e - Q_t)^2 \tag{3}$$

$$Q_t = \frac{1}{\beta}\ln(\alpha\beta) + \frac{1}{\beta}\ln t \tag{4}$$

$$Q_t = k_d t^{1/2} + c_i \tag{5}$$

where Q_t and Q_e were the corresponding adsorptive quantities at t time and adsorption equilibrium respectively, mg·g^{-1}. k_1 (min^{-1}), k_2 (g mg^{-1} min^{-1}) and k_d (mg g^{-1} min$^{-1/2}$) were the rate constant of the pseudo first order equation, the rate constant of the pseudo second order equation and apparent diffusion rate constants, respectively. α (mg g^{-1} min^{-1}) and β (g mg^{-1}) were the initial adsorption rate constant and a parameter of the Elovich equation, respectively. β was related to the extent of surface coverage and activation energy for chemisorption. c_i (mg g^{-1}) was a constant representing the thickness of the liquid film.

The Langmuir mode (Eq. 6), the Freundlich model (Eq. 7) and the Temkin model (Eq. 8) were used to fit the isothermal adsorption process of Zn^{2+} adsorption on biochars, and the equations for each model were as follows [3-5]:

$$Q_e = \frac{Q_m K_L C_e}{1 + K_L C_e} \tag{6}$$

$$Q_e = K_F C_e^{1/n} \tag{7}$$

$$Q_e = A \ln K_T C_e \tag{8}$$

where C_e (mg L^{-1}), Q_e (mg g^{-1}) and Q_m (mg g^{-1}) were the concentration of Zn^{2+} at equilibrium, adsorption capacity of Zn^{2+} at equilibrium, and the saturated adsorption capacity for monolayer adsorption, respectively. K_L (L mg^{-1}), K_F [mg$^{(1-1/n)}$ L$^{1/n}$ g^{-1}] and K_T (L mg^{-1}) were the adsorption coefficient of the Langmuir mode, the Freundlich model and Temkin model. The dimensionless constant n represented the adsorption intensity or surface heterogeneity. A (kJ mol^{-1}) was a coefficient related to the heat of adsorption.

The quality of adsorbent and whether it can absorb pollutants effectively could be judged by dimensionless parameter, separation factor (R_L). R_L was considered as more reliable indicator of the adsorption. The equation for calculating R_L was as follows [3-5]:

$$R_L = \frac{1}{1 + K_L c_0} \tag{9}$$

where K_L and C_0 were the Langmuir constant and the initial Zn^{2+} concentration. There were four possibilities for the value of R_L, 0-1, greater than 1, equal to 1 and equal to 0, which indicated that the adsorption process of adsorbent to adsorbate belongs to favorable adsorption, unfavorable adsorption, linear adsorption and irreversible adsorption, respectively.

Theoretical calculation method of the G09 package

The binding energy between the heavy metal ions (Ca^{2+}, Mg^{2+} or Zn^{2+}) and the benzene ring, catechol or phthalic acid were calculated using the G09 package. M^{2+}-C_6H_6, M^{+}-$C_6H_5O_2$ or M^{+}-$C_6H_5O_4$ complexes were calculated at the B3LYP/6-311+G** level (M= Ca, Mg or Zn). The binding energy between the heavy metal ions (Ca^{2+}, Mg^{2+} and Zn^{2+}) and the benzene ring, catechol or phthalic was calculated by as follows:

$$\Delta E = E_{oc} + E_M - E_{oc\text{-}M}$$

where $\triangle E$ (eV) is the binding energy between M^{2+} and the benzene ring, catechol or phthalic acid. E_{oc} (eV) is the the total energy of the organic compounds including the benzene ring, catechol and phthalic acid. E_M (eV) is the the total energy of the Ca^{2+}, Mg^{2+} or Zn^{2+}, respectively. $E_{oc\text{-}M}$ (eV) is the total energy of the M^{2+}-C_6H_6, M^{+}-$C_6H_5O_2$ and M^{+}-$C_6H_5O_4$ complexes.

Table S1 Comparison of the adsorption capacities of Zn^{2+} by different types of biochars

Feedstock	Pyrolysis temperature of biochar/ °C	Q_m/ mg g^{-1}	References
rice straw	550	39.7	[10]
chicken manure	550	11.2	
sewage sludge	550	4.3	
rice straw	600	40.2	[11]
wheat straw	650-700	41.8	[12]
S. hermaphrodita	700	48.1	
hardwood	450	4.5	[13]
corn straw	600	11.0	
dead carp	450-650	80.7-87.7	This study

Q_m is the maximum monolayer adsorption capacities based on Langmuir model, mg g^{-1}.

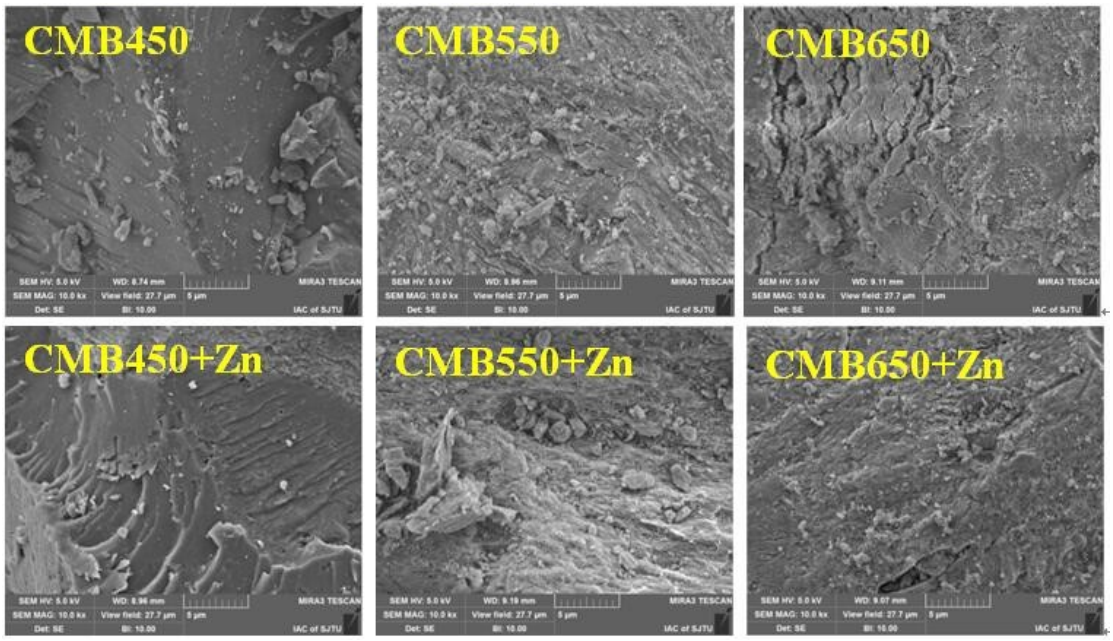

Fig. S1 SEM images of biochars (CMB450, CMB550 and CMB650) and Zn loaded biochars (CMB450+ Zn, CMB550+ Zn and CMB650+Zn).

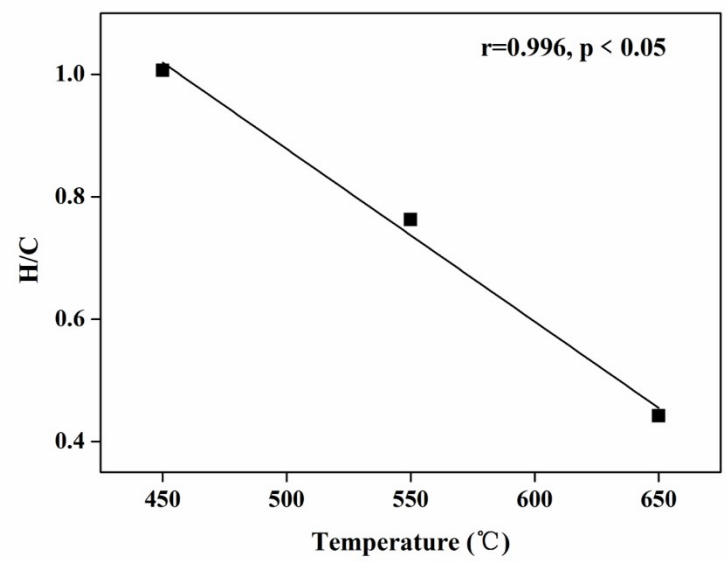

Fig. S2 Correlations between the pyrolysis temperature and O/C.

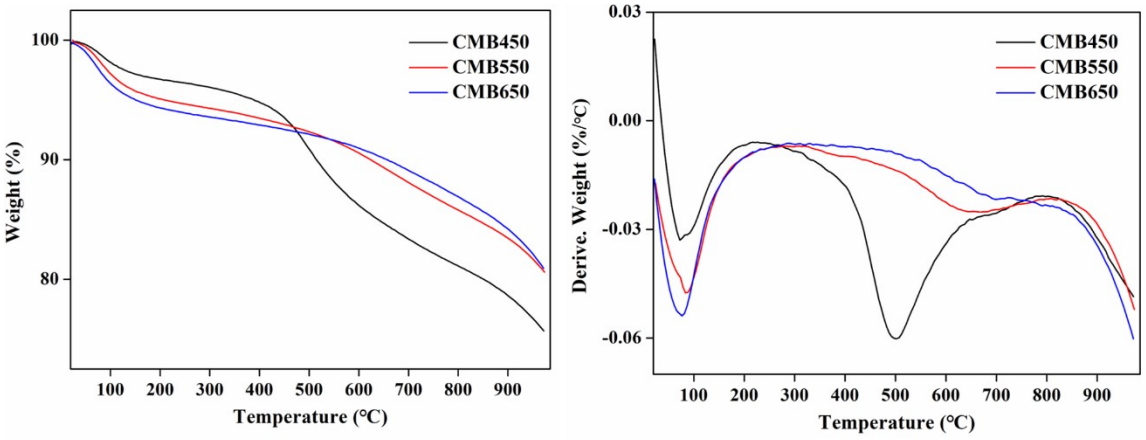

Fig. S3 Thermogravimetric and differential thermal gravimetric curves of biochars (CMB450, CMB550 and CMB650).

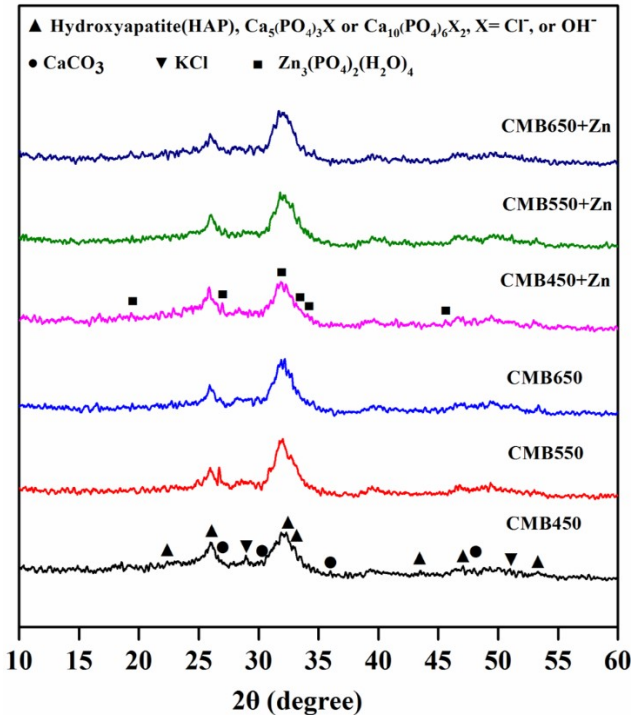

Fig. S4 XRD patterns of biochars (CMB450, CMB550 and CMB650) and Zn loaded biochars (CMB450+Zn, CMB550+Zn and CMB650+Zn).

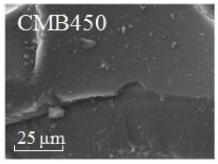

Element	CMB450									
	C	N	O	Na	Mg	P	S	Cl	K	Ca
Wt %	73.16	10.46	10.32	0.52	0.25	1.60	0.21	0.10	2.95	0.43
Atomic %	79.60	9.76	8.43	0.29	0.13	0.68	0.09	0.04	0.84	0.14

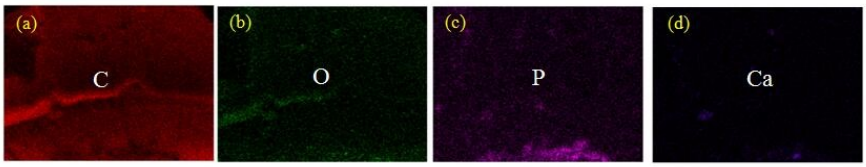

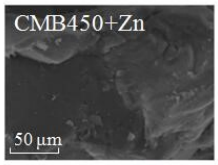

Element	CMB450+Zn						
	C	O	Na	P	Mg	Ca	Zn
Wt %	32.4	30.03	0.47	11.12	0.36	25.17	0.46
Atomic %	48.14	33.50	0.36	6.41	0.26	11.21	0.13

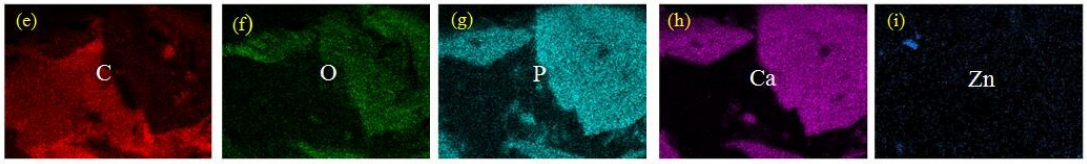

Fig. S5 SEM images of CMB450 and CMB450+Zn (Zn loaded biochars), and elemental dot maps of CMB450 (a-d) and CMB450+ Zn (e-i) scanned in the region CMB450 and CMB450+Zn by EDS, respectively. The mass percentages (Wt %) and atomic percentages (Atomic %) of elements were listed in the table. The Zn dot map of CMB450 loaded with Zn^{2+} (i) and weight percentage of Zn in the CMB450+Zn (0.46 %) indicated that Zn^{2+} was adsorbed onto CMB450. The Zn dot of CMB550+Zn (i) was coincident with the O dot (f) and P dot (g), implying complexation of Zn^{2+} with oxygen-containing functional groups occurred or Zn-phosphate possibly formed.

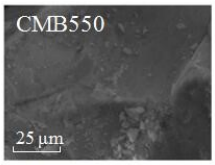

Element	CMB550								
	C	O	Na	Mg	Al	P	Cl	K	Ca
Wt %	22.01	35.77	0.83	0.38	0.16	10.58	0.66	1.69	27.91
Atomic %	35.07	42.78	0.69	0.30	0.12	6.54	0.36	0.83	13.32

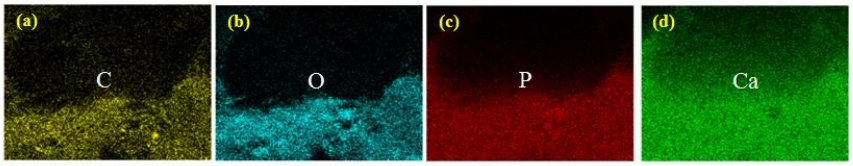

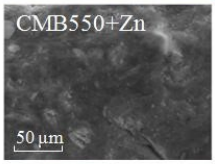

Element	CMB550+Zn						
	C	O	Na	Mg	P	Ca	Zn
Wt %	11.54	33.47	1.35	0.22	15.59	27.15	10.67
Atomic %	21.52	46.86	1.31	0.21	11.27	15.17	3.66

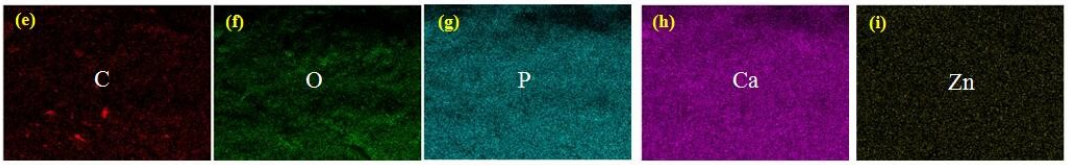

Fig. S6 SEM images of CMB550 and CMB550+Zn (Zn loaded biochars), and elemental dot maps of CMB550 (a-d) and CMB550+Zn (e-i) scanned in the region CMB550 and CMB550+Zn by EDS, respectively. The mass percentages (Wt %) and atomic percentages (Atomic %) of elements were listed in the table. The Zn dot map of CMB550 loaded with Zn^{2+} (i) and weight percentage of Zn in the CMB550+Zn (10.67 %) indicated that Zn^{2+} was adsorbed onto CMB550.

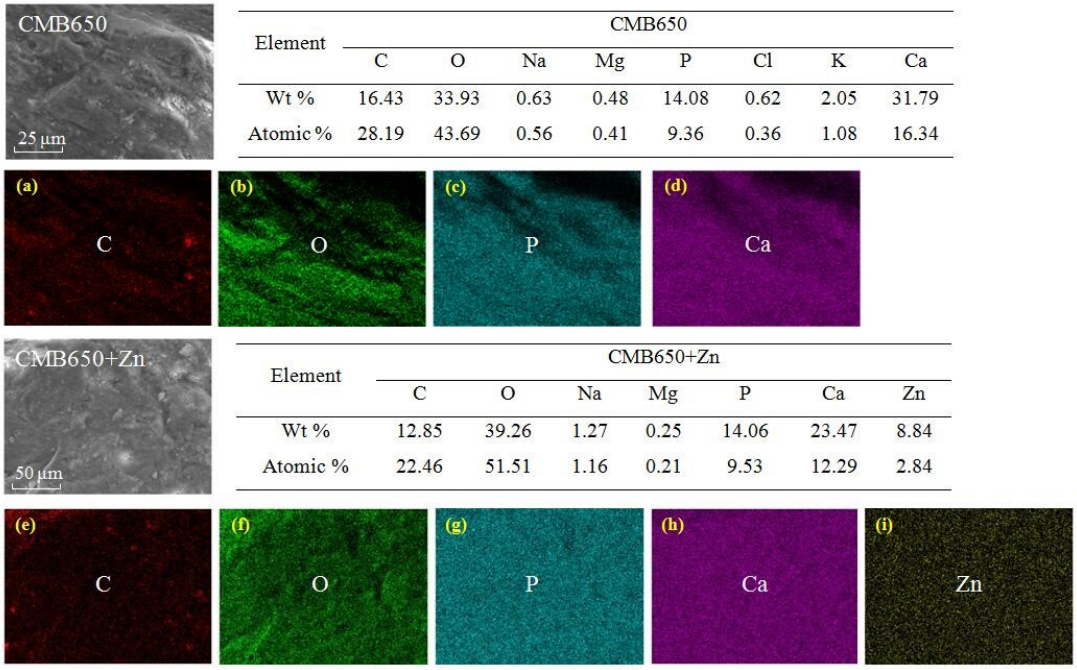

Element	CMB650							
	C	O	Na	Mg	P	Cl	K	Ca
Wt %	16.43	33.93	0.63	0.48	14.08	0.62	2.05	31.79
Atomic %	28.19	43.69	0.56	0.41	9.36	0.36	1.08	16.34

Element	CMB650+Zn						
	C	O	Na	Mg	P	Ca	Zn
Wt %	12.85	39.26	1.27	0.25	14.06	23.47	8.84
Atomic %	22.46	51.51	1.16	0.21	9.53	12.29	2.84

Fig. S7 SEM images of CMB650 and CMB650+Zn (Zn loaded biochars), and elemental dot maps of CMB650 (a-d) and CMB650+Zn (e-i) scanned in the region CMB650 and CMB650+Zn by EDS, respectively. The mass percentages (Wt %) and atomic percentages (Atomic %) of elements were listed in the table. The Zn dot map of CMB650 loaded with Zn^{2+} (i) and weight percentage of Zn in the CMB450+Zn (8.84 %) indicated that Zn^{2+} was adsorbed onto CMB650.

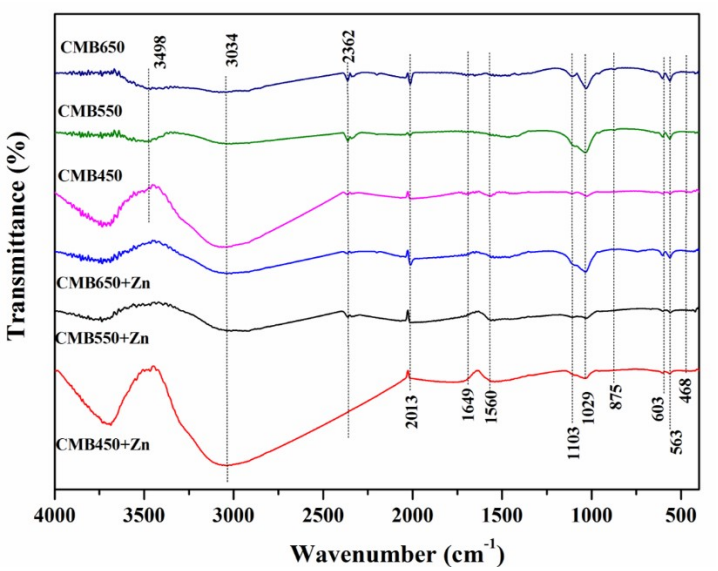

Fig. S8 FTIR spectra of biochars (CMB450, CMB550 and CMB650) and Zn loaded biochars (CMB450+Zn, CMB550+Zn and CMB650+Zn). The bands at 2013, 1029, 563 and 468 cm^{-1} were attributed to the v_1, v_3, v_4 and v_2 modes of PO_4^{3-} [6-7], respectively. The bands 875 cm^{-1} was attributed to CO_3^{2-} [7]. In addition, biochars also contained more organic functional groups, including phenolic-OH (3498 cm^{-1}), CO-OH (3034 cm^{-1}), N-H (2362 cm^{-1}), C=C (1649 cm^{-1}), C-O-C (1103 cm^{-1}), and C=O (1560 cm^{-1}) [7-9].

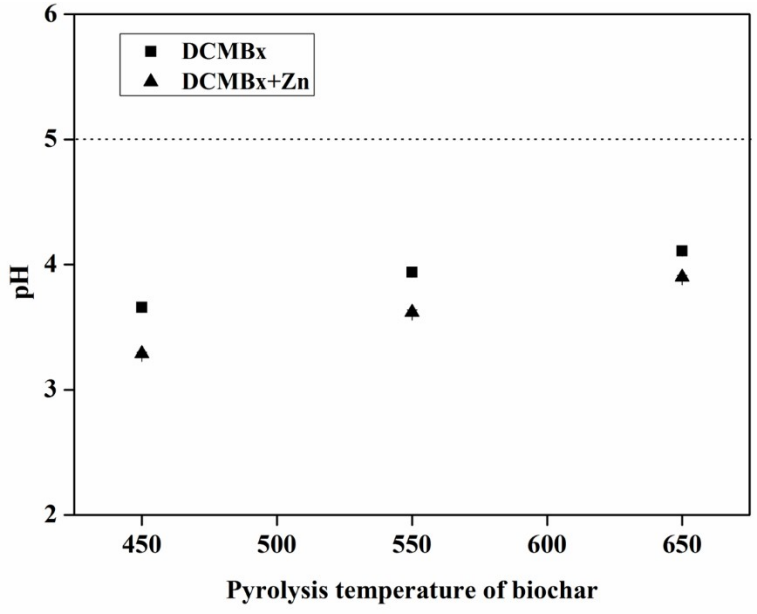

Fig. S9. The pH change of the mixed solution of DCMBx with and without (marked as the blank systems) Zn^{2+} after equilibration.

References

[1] Gao L Y, Deng J H, Huang G F, et al. Relative distribution of Cd^{2+} adsorption mechanisms on biochars derived from rice straw and sewage sludge[J]. Bioresour. Technol. 2019, 272: 114-122.

[2] Lee S J, Park J H, Ahn Y T, et al. Comparison of heavy metal adsorption by peat moss and peat moss-derived biochar produced under different carbonization conditions[J]. Water Air Soil Pollut. 2015, 226: 1-11.

[3] Wang Z, Liu G, Zheng H, et al. Investigating the mechanisms of biochar's removal of lead from solution[J]. Bioresour. Technol. 2015, 177: 308-17.

[4] Deng Y, Huang S, Larid DA, et al. Adsorption behaviour and mechanisms of cadmium and nickel on rice straw biochars in single- and binary-metal systems[J]. Chemosphere. 2019, 218: 308-318.

[5] Tran H N, You S J, Hosseini-Bandegharaei A, et al. Mistakes and inconsistenciesregarding adsorption of contaminants from aqueous solutions: A critical review[J]. Water Res. 2017, 120: 88-116.

[6] Markovic M, Fowler B O, Tung M S. Preparation and comprehensive characterization of a calcium hydroxyapatite reference material[J]. J. Res. Natl. Inst. Stand. Technol. 2004, 109: 553-568.

[7] Lei S, Shi Y, Qiu Y, et al. Performance and mechanisms of emerging animal-derived biochars for immobilization of heavy metals[J]. Sci. Total Environ. 2019, 646: 1281-1289.

[8] Koutsopoulos S. Synthesis and characterization of hydroxyapatite crystals: a review study on the analytical methods[J]. J. Biomed. Mater. Res. 2002, 62: 600-612.

[9] Wang Z, Shen S, Shen D, et al. Immobilization of Cu^{2+} and Cd^{2+} by earthworm manure derived biochar in acidic ircumstance[J]. J. Environ. Sci. 2017, 53: 93-300.

[10] M. Zhao, Y. Dai, M. Zhang, C. Feng and R. Qiu, Sci. Total Environ., 2020, 717, 136894. https://doi.org/10.1016/j.scitotenv.2020.136894.

[11] J. H. Park, J. J. Wang, S. H. Kim, J. S. Cho, S. W. Kang, R. D. Delaune, K. J. Han and D. C. Seo, Colloid. Surface. A, 2017, 533, 330-337.

[12] A. Bogusz, P. Oleszczuk and R. Dobrowolski, Bioresour. Technol., 2015, 196, 540-549.

[13] X. Chen, G. Chen, L. Chen, Y. Chen, J. Lehmann, M. B. McBride and A. G. Hay, Bioresour. Technol., 2011, 102, 8877-8884.